

Topology meets MOF Chemistry for pore-aperture fine tuning: ftw-MOF platform for energy-efficient separations via adsorption kinetics or molecular sieving

Dong-Xu Xue, Amandine Cadiou, Łukasz J. Weseliński, Hao Jiang, Prashant M. Bhatt, Aleksander Shkurenko, Lukasz Wojtas, Chen Zhijie, Youssef Belmabkhout, Karim Adil, Mohamed Eddaoudi*

Table of Contents

1. Material and methods.....	2
2. Synthesis and activation of 1 and 2.....	8
3. Single crystal data.....	10
4. Powder X-ray Diffraction Patterns	13
5. Variable temperature powder diffraction.....	15
6. TGA analysis	16
7. Low-Pressure Gas Adsorption Measurements.....	17
8. Breakthrough experiments.....	23
9. High-Pressure Gas Adsorption Measurements	24
10. References.....	27

1. Material and methods

Analyses for C, H and N were carried out on a ThermoFinnigan Apparatus.

Thermal gravimetric analyses (TGA) were performed under N₂ flow (25 ml/min) with a heating rate of 5°C/min using a TA Q500 apparatus.

TGA-DSC

Enthalpy of adsorption for propane and propylene were measured using SENSYS evo TG-DSC from Setaram Instrumentation that can carry out simultaneous high resolution DSC and TGA experiments. In a typical experiment, the sample was activated in-situ at 160 °C under continuous dry N₂ flow at the rate of 15 ml/min. For sorption experiment, baseline was obtained under dry N₂ flow at the rate of 15ml/min at 25 °C. Propane or propylene was connected at auxiliary gas port and gas was changed from N₂ to propane/propylene exactly after 0.5 hour and TGA and DSC signal were monitored for few hours to obtain uptake and heat of sorption respectively.

The powder X-ray pattern and the variable humidity powder X-ray diffraction data (PXRD) were collected over the 2θ range 4–40° on a high resolution PANalytical X'Pert MPD-PRO diffractometer with Cu $K\alpha$ radiation ($\lambda = 1.5406 \text{ \AA}$, 45 kV/40 mA) equipped with the humidity controller.

Variable Temperature Powder X-ray Diffraction (VT-PXRD) measurements were collected on a PANalyticalX'Pert MPD-PRO X-ray diffractometer equipped with an Anton-Parr CHC+ variable temperature stage. Measurements were collected at 45 kV, 40 mA for Cu $K\alpha$ ($\lambda = 1.5418 \text{ \AA}$) with a scan speed of $1.0^\circ \text{ min}^{-1}$ and a step size of 0.02° in 2θ . Samples were placed under vacuum during analysis and analysis and the sample was held at the designated temperatures for at least 15 minutes between each scan.

X-ray Single Crystal Diffraction data were collected on a Bruker X8 PROSPECTOR APEX2 CCD diffractometer using Cu $K\alpha$ radiation ($\lambda = 1.54178 \text{ \AA}$). Indexing was performed using APEX2 (Difference Vectors method).¹

Data integration and reduction were performed using SaintPlus 8.34.² Absorption correction was performed by multi-scan method implemented in SADABS.³ Space group was determined using XPREP implemented in APEX2. Structure was solved using Direct Methods (SHELXS-97) and refined using SHELXL-97 (full-matrix least-squares on F^2) contained WinGX v1.70.01 (**1**)⁴ and Olex2⁵ (**2**). Crystal data and structure refinement conditions for crystal structures **1** and **2** are summarized in Tables S1 and S2, respectively.

Low-pressure gas sorption measurements were performed on a fully automated Quadrasorb SI (for CO₂ sorption screening) and Autosorb-iQ gas adsorption analyzer, (Quantachrome Instruments) at relative pressures up to 1 atm. The bath temperature for the CO₂ sorption measurements was controlled using an ethylene glycol/H₂O re-circulating bath.

High-pressure gas adsorption studies were performed on a magnetic suspension balance marketed by Rubotherm (Germany) (Scheme S1), composed mainly of a magnetic suspension balance (MSB) and a network of valves, mass flow meters, and temperature and pressure sensors. The MSB overcomes the disadvantages of other commercially available gravimetric instruments by separating the sensitive microbalance from the sample and the measuring atmosphere, and is able to perform adsorption measurements across a wide pressure range (i.e., from 0 to 20 MPa). The adsorption temperature may also be controlled within the range of 77 K to 423 K. In a typical adsorption experiment, the adsorbent is precisely weighed and placed in a basket suspended by a permanent magnet through an electromagnet. The cell in which the basket is housed is then closed and vacuum or high pressure is applied. The gravimetric method allows the direct measurement of the reduced gas adsorbed amount (Ω). Correction for the buoyancy effect is required to determine the excess

and absolute adsorbed amount using equations 1 and 2, where $V_{adsorbent}$ and V_{ss} and $V_{adsorbed\ phase}$ refer to the volume of the adsorbent, the volume of the suspension system, and the volume of the adsorbed phase, respectively.

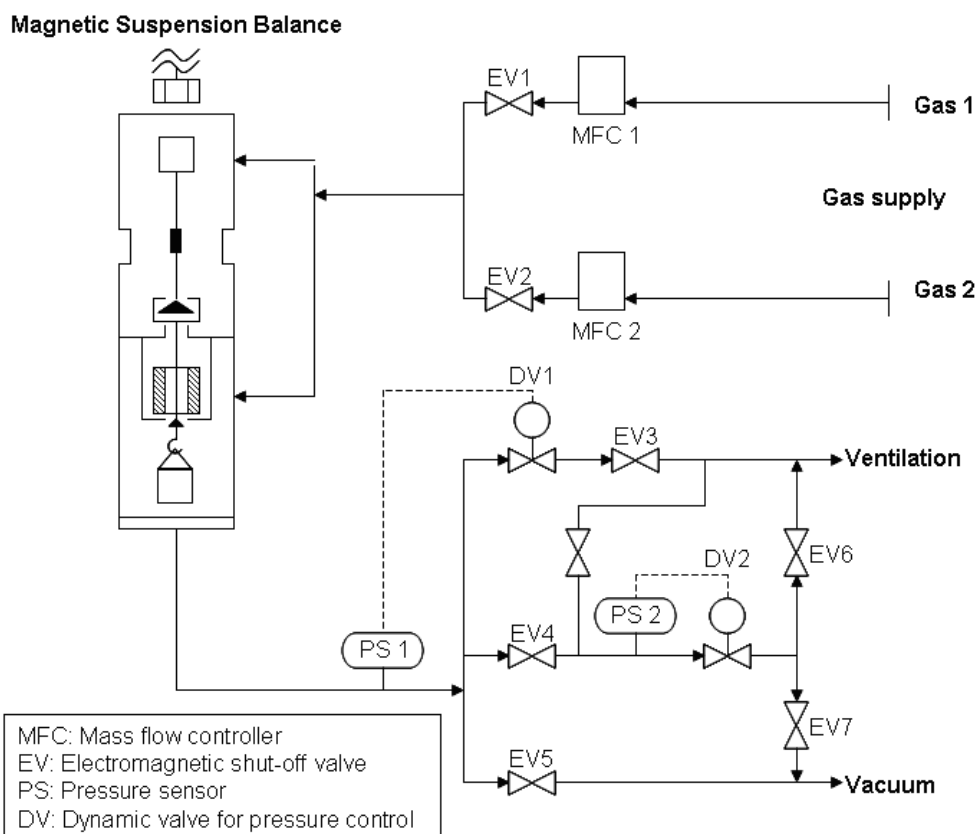
$$\Omega = m_{absolute} - \rho_{gas}(V_{adsorbent} + V_{ss} + V_{adsorbed\ phase}) \quad (1)$$

$$\Omega = m_{excess} - \rho_{gas}(V_{adsorbent} + V_{ss}) \quad (2)$$

The buoyancy effect resulting from the adsorbed phase may be taken into account via correlation with the pore volume or with the theoretical density of the sample.

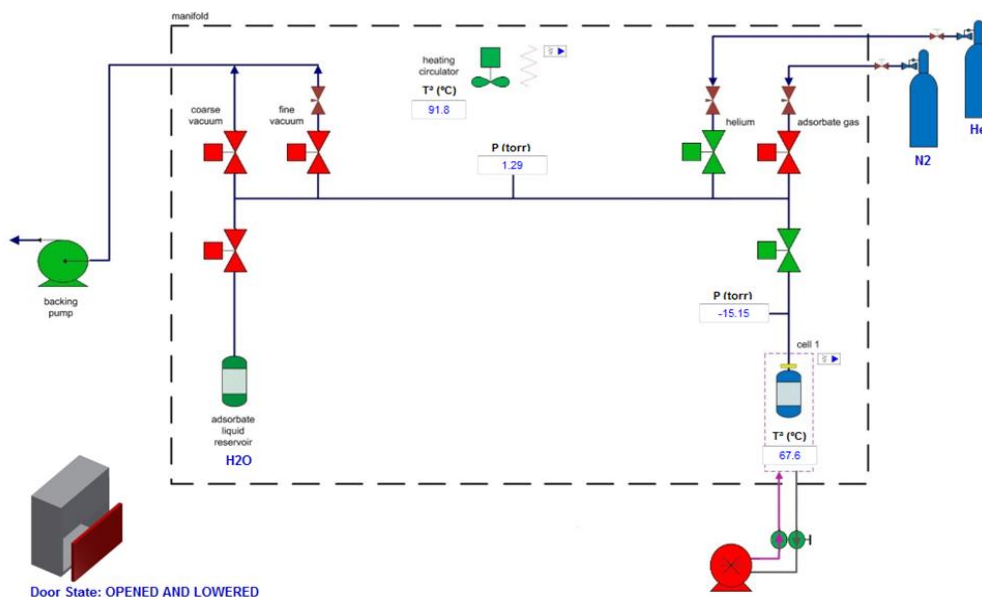
These volumes are determined using the helium isotherm method by assuming that helium penetrates in all open pores of the materials without being adsorbed. The density of the gas is determined using the Refprop equation of state (EOS) database and checked experimentally using a volume-calibrated titanium cylinder. By weighing this calibrated volume in the gas atmosphere, the local density of the gas is also determined. Simultaneous measurement of adsorption capacity and gas-phase density as a function of pressure and temperature is therefore possible.

The pressure is measured using two Druck's high-pressure transmitters ranging from 0.5 to 34 bar and 1 to 200 bar, respectively, and one low pressure transmitter ranging from 0 to 1 bar. Prior to each adsorption experiment, about 200 mg of sample is outgassed at 373 K at a residual pressure of 10–6 mbar. The temperature during adsorption measurements is held constant by using a thermostat-controlled circulating fluid.



Scheme S1. Representation of the Rubotherm gravimetric-densimetric apparatus.

Vstar1 vapor sorption analyzer from Quantachrome instruments was used for propane/propylene sorption (Scheme S2). In a typical experiment, sample was activated in-situ at 160°C under dynamic vacuum for 8 hours. Temperature was increased to 160°C from room temperature at the rate of 1°C/min. Activated sample was used for corresponding isotherm measurement. All the sorption experiments were carried out at 20°C sample temperature unless otherwise mentioned. Manifold temperature was maintained at 40 °C throughout the measurement. Sorption data were processed by using Helmholtz equation.

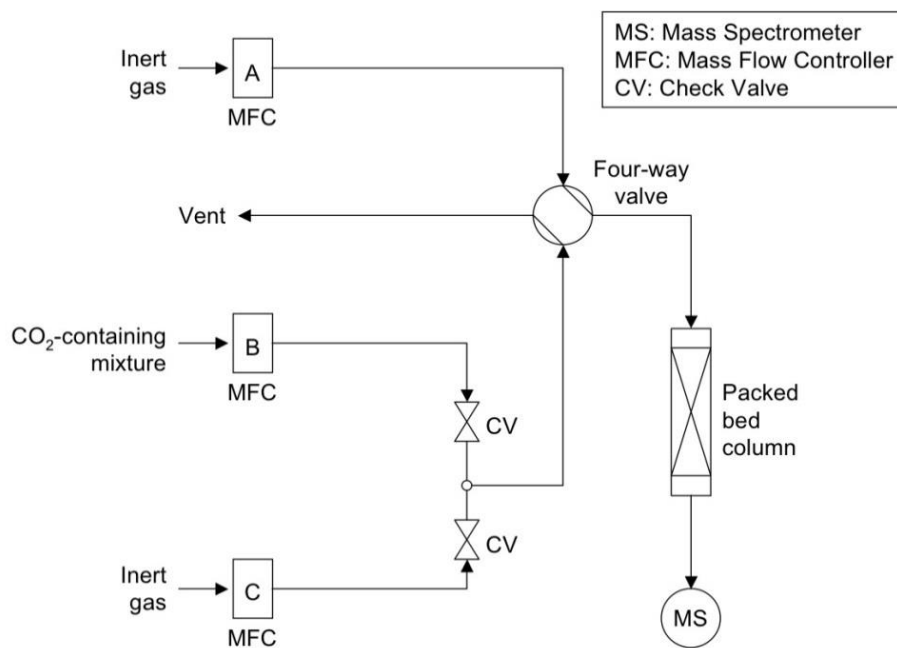


Scheme S2. Schematic diagram of Vstar1 vapor sorption analyzer.

Column Breakthrough Test Set-up, Procedure and Measurements:

The experimental set-up used for dynamic breakthrough measurements is shown in Scheme 3. The gas manifold consisted of three lines fitted with mass flow controllers. Line “A” is used to feed an inert gas, most commonly helium, to activate the sample before each experiment. The other two lines, “B” and “C” feed a pure or pre-mixed gases. Whenever required, gases flowing through lines “B” and “C” may be mixed before entering a column packed with **2** using a four-way valve. In a typical experiment, 1.49g of adsorbent (in the column) was treated at 433 K overnight under vacuum in a separate oven.

After the sample is degassed, the column is backfilled with argon and mounted in the set-up. Before starting each experiment, helium reference gas is flushed through the column and then the gas flow is switched to the desired gas mixture at the same flow rate of 6 cc/min (11 cc/min for $C_3H_8/C_3H_6/N_2:5/5/90$). The gas mixture downstream the column was monitored using a Hiden mass-spectrometer.

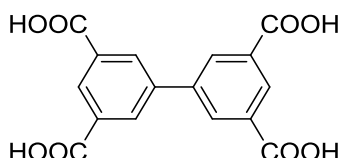


Scheme S3. Representation of the column breakthrough experiment.

2. Synthesis and activation of 1 and 2.

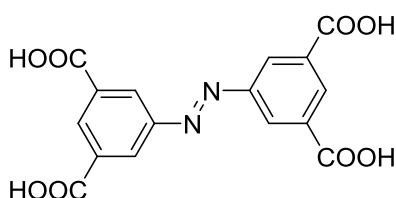
All reagents were used as received unless otherwise stated from Fisher Scientific, Acros Organics, Combi-Blocks, AK Scientific, Sigma-Aldrich, or TCI America. DI water = deionized water. ^1H and ^{13}C NMR spectra were recorded at room temperature with Bruker Avance 500 and 600 MHz spectrometers using DMSO-d_6 as a solvent, and referenced to the corresponding solvent peaks (2.50 and 39.52 ppm, respectively).

Synthesis of biphenyl-3,3',5,5'-tetracarboxylic acid (H_4BPTC)



In a 500 ml Schlenk tube, a mixture of acetonitrile (50 ml) and aq. K_2CO_3 (12.4 g, 90 mmol in 50 ml DI water) was prepared and the tube was evacuated/backfilled with argon 3x, then dimethyl 5-bromoisophthalate (3 g, 11 mmol), 3,5-dicarboxybenzeneboronic acid (2.1 g, 10 mmol) and $\text{Pd}(\text{PPh}_3)_2\text{Cl}_2$ (400 mg, 0.57 mmol) were added, the tube was evacuated/backfilled with argon 3x, then sealed and heated at $100\text{ }^\circ\text{C}$ (oil bath) for 4 d with vigorous stirring. Then the mixture was diluted with DI water (100 ml) and stirred at the same temperature for 24 h. The reaction mixture was then cooled and filtered through Celite®, washing with additional aq. NaHCO_3 . The filtrate was washed with AcOEt (100 ml, discarded), diluted with DI water to 600 ml total volume, and carefully (effervescence!) acidified with aq. HCl to pH ~ 2. The precipitated solid was filtered on paper, washed thoroughly with DI water and dried on air overnight to give white solid, 2.6 g (79%). NMR data match the reported values. ⁶

Synthesis of azobenzene-3,3',5,5'-tetracarboxylic acid (H_4ABTC)



It was obtained according to the reported procedure in sufficient purity as an orange solid. ⁷

Synthesis of Y-biphenyl-ftw (1)

$\text{Y}(\text{NO}_3)_2 \cdot 9\text{H}_2\text{O}$ (35.3 mg, 0.092 mmol, Aldrich), H_4BPTC (3.6 mg, 0.011 mmol) and 2-fluorobenzoic acid (642.1 mg, 4.58 mmol, Aldrich) were mixed and dispersed in a mixture of DMF (2 mL), deionized water (0.5 mL) and HNO_3 3.5M in water (0.15 mL) into a pyrex tube. The tube was then sealed and heated to 115C° for 24 h. After cooling down, the resulting colorless square shape crystals, suitable for single crystal structure determination, were separated by filtration, washed with ethanol and dried in air.

1 was exchanged for 3 days in ethanol at room temperature then filtrated before being evacuated at 125°C under vacuum (3 milliTorrs) in order to performed sorption measurements.

Synthesis of Tb-ABTC-ftw (2)

H₄ABTC (7.88 mg, 0.022 mmol), Tb(NO₃)₃·6H₂O (19.7 mg, 0.0435 mmol), 2-fluorobenzoic acid (243.6 mg, 1.74 mmol), DMF (1.7 mL), and HNO₃ (0.3 mL, 3.5 M in DMF) were combined in a 20 mL scintillation vial, sealed and heated to 115°C for 60 h and cooled to room temperature. The colorless cubic crystals were collected, washed with DMF and then air-dried.

2 was exchanged for 3 days in methanol at room temperature then filtrated before being evacuated at 160°C under vacuum (3 milliTorrs) in order to performed sorption measurements.

3. Single crystal data

Compounds **1** and **2** crystallize in the cubic $Im\bar{3}$ space group and the trigonal space group $R\bar{3}c$, respectively. Both structures **1** and **2** are isorecticular. $[RE_6(OH)_8]$ building blocks are bridged by biphenyltetracarboxylate (BPTC) or diazobenzenetetracarboxylate (ABTC) anions forming **ftw** framework. Each BPTC anion moiety in **1** is twisted and disordered over 2 positions with the equal occupancy of 0.5. Large set of restraints and constraints was applied to make both geometry and thermal parameters of the spacer anions reasonable. Strongly disordered dimethylammonium (DMA) cations, dimethylformamide (DMF) and water molecules were localised in the pores. DMA and DMF were refined isotropically with no restraints applied to their thermal parameters (only to interatomic distances, DFIXes). ABTC anions in **2** are ordered and refined anisotropically. DMA, DMF and water molecules were refined isotropically with a set of restraints applied to DMA and DMF geometry and thermal parameters.

Crystal structure **1** was refined as a 2-component merohedral twin with the twin law $-1\ 0\ 0\ 0\ 0\ 1\ 0\ 1\ 0$ and fractional contributions of ~ 0.5 using SHELXL-2014/7. The pseudo-merohedral twin **2** was detwinned by integration software (SAINT v8.34A, Bruker, 2013). Hydrogen atoms are placed at calculated positions and refined using a riding model in both **1** and **2**. The PLATON's SQUEEZE procedure was applied to estimate diffuse electron density of heavily disordered solvent molecules in the cavities of **1** but the structure factors were not corrected for the solvent contribution.

Table S1. Crystal data and structure refinement conditions for **1**.

Empirical formula	C ₅₅ H ₆₀ N ₃ O _{38.5} Y ₆
Formula weight	1912.52
Crystal system, space group	Cubic, <i>Im</i> -3
Unit cell dimensions	$a = 25.1402(7) \text{ \AA}$
Volume	15889(1)
Z, calculated density	8, 1.599 Mg m ⁻³
$F(000)$	7624
Temperature (K)	100(1)
Radiation type, λ	Cu $K\alpha$
Absorption coefficient	6.40 mm ⁻¹
Absorption correction	Multi-scan
Max and min transmission	0.051 and 0.146
Crystal size	0.02 × 0.02 × 0.02 mm
Shape, color	Cubic, colorless
θ range for data collection	2.5–64.2°
Limiting indices	$-29 \leq h \leq 29, -29 \leq k \leq 29, -29 \leq l \leq 29$
Reflection collected / unique / observed with $I > 2\sigma(I)$	28451 / 2383 ($R_{\text{int}} = 0.078$) / 2157
Completeness to $\theta_{\text{max}} = 64.2^\circ$	99.9 %
Refinement method	Full-matrix least-squares on F^2
Data / restraints / parameters	2383 / 168 / 211
Final R indices [$I > 2\sigma(I)$]	$R_1 = 0.125, wR_2 = 0.310$
Final R indices (all data)	$R_1 = 0.150, wR_2 = 0.334$
Weighting scheme	$[\sigma^2(F_o^2) + (0.2P)^2]^{-1*}$
Goodness-of-fit	1.17
Largest diff. peak and hole	5.81 and -1.28 e \AA^{-3}

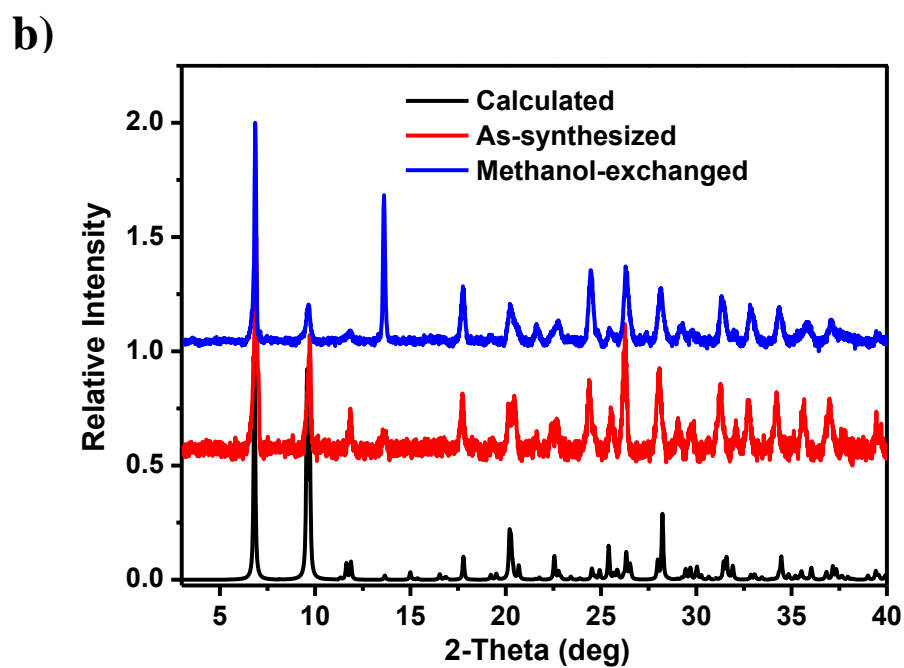
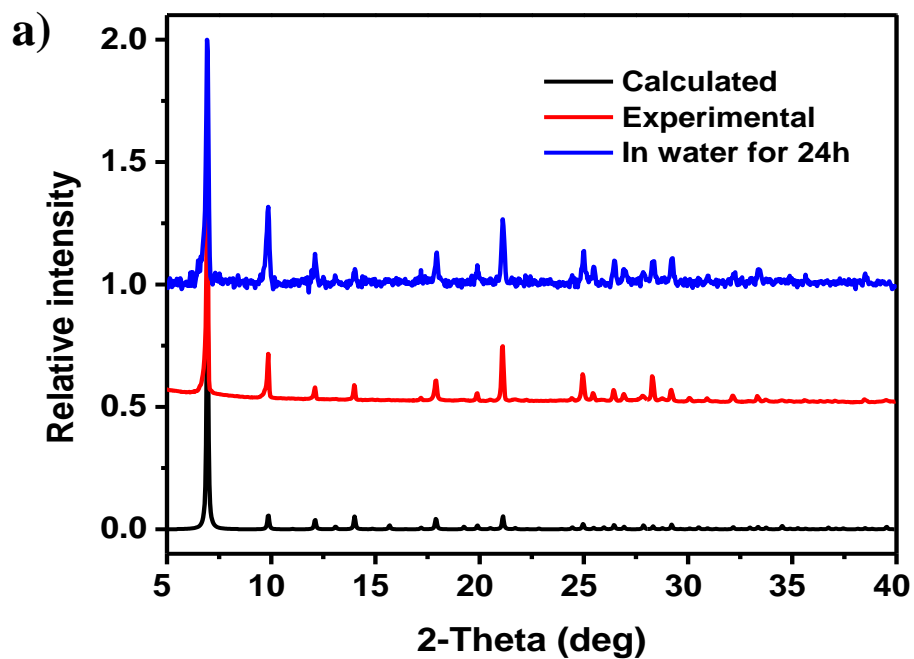
* $P = (F_o^2 + 2F_c^2)/3$

Table S2. Crystal data and structure refinement conditions for **2**.

Empirical formula	C _{56.5} H ₅₉ N _{9.5} O _{36.75} Tb ₆
Formula weight	2412.59
Crystal system, space group	Trigonal, <i>R</i> -3 <i>c</i>
Unit cell dimensions	<i>a</i> = 18.232(1) Å, <i>c</i> = 45.607(3) Å
Volume	13130(2)
Z, calculated density	6, 1.831 Mg m ⁻³
<i>F</i> (000)	6891
Temperature (K)	100(1)
Radiation type, λ	Cu <i>K</i> α
Absorption coefficient	24.04 mm ⁻¹
Absorption correction	Multi-scan
Max and min transmission	0.622 and 0.753
Crystal size	0.01 × 0.02 × 0.06 mm
Shape, color	Rod, colorless
θ range for data collection	3.4–70.3°
Limiting indices	-22 ≤ <i>h</i> ≤ 11, 0 ≤ <i>k</i> ≤ 22, 0 ≤ <i>l</i> ≤ 55
Reflection collected / unique / observed with <i>I</i> > 2σ(<i>I</i>)	5090 / 2744 (<i>R</i> _{int} = 0.026) / 2425
Completeness to $\theta_{\max} = 70.3^\circ$	98.3 %
Refinement method	Full-matrix least-squares on <i>F</i> ²
Data / restraints / parameters	2744 / 23 / 187
Final <i>R</i> indices [<i>I</i> > 2σ(<i>I</i>)]	<i>R</i> ₁ = 0.043, <i>wR</i> ₂ = 0.115
Final <i>R</i> indices (all data)	<i>R</i> ₁ = 0.051, <i>wR</i> ₂ = 0.119
Weighting scheme	[$\sigma^2(F_o^2) + (0.0561P)^2 + 280.1767P$] ^{-1*}
Goodness-of-fit	1.12
Largest diff. peak and hole	0.96 and -0.97 e Å ⁻³

* $P = (F_o^2 + 2F_c^2)/3$

4. Powder X-ray Diffraction Patterns



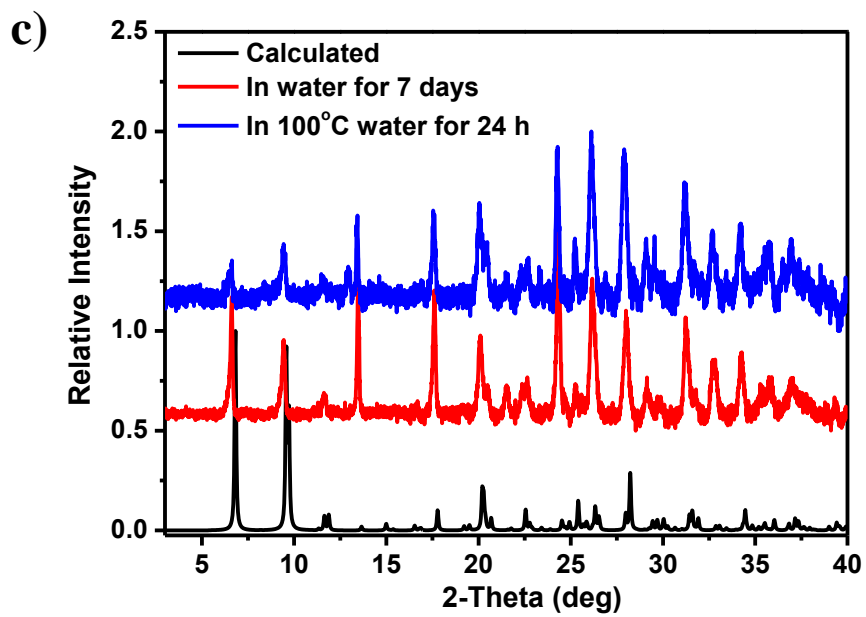


Figure S1. PXRD patterns of a) calculated, as-synthesized and after 24h in water of **1**, b) calculated, as-synthesized and solvent-exchanged **2**, c) after soaking at room temperature and boiling water of **2**.

5. Variable temperature powder diffraction

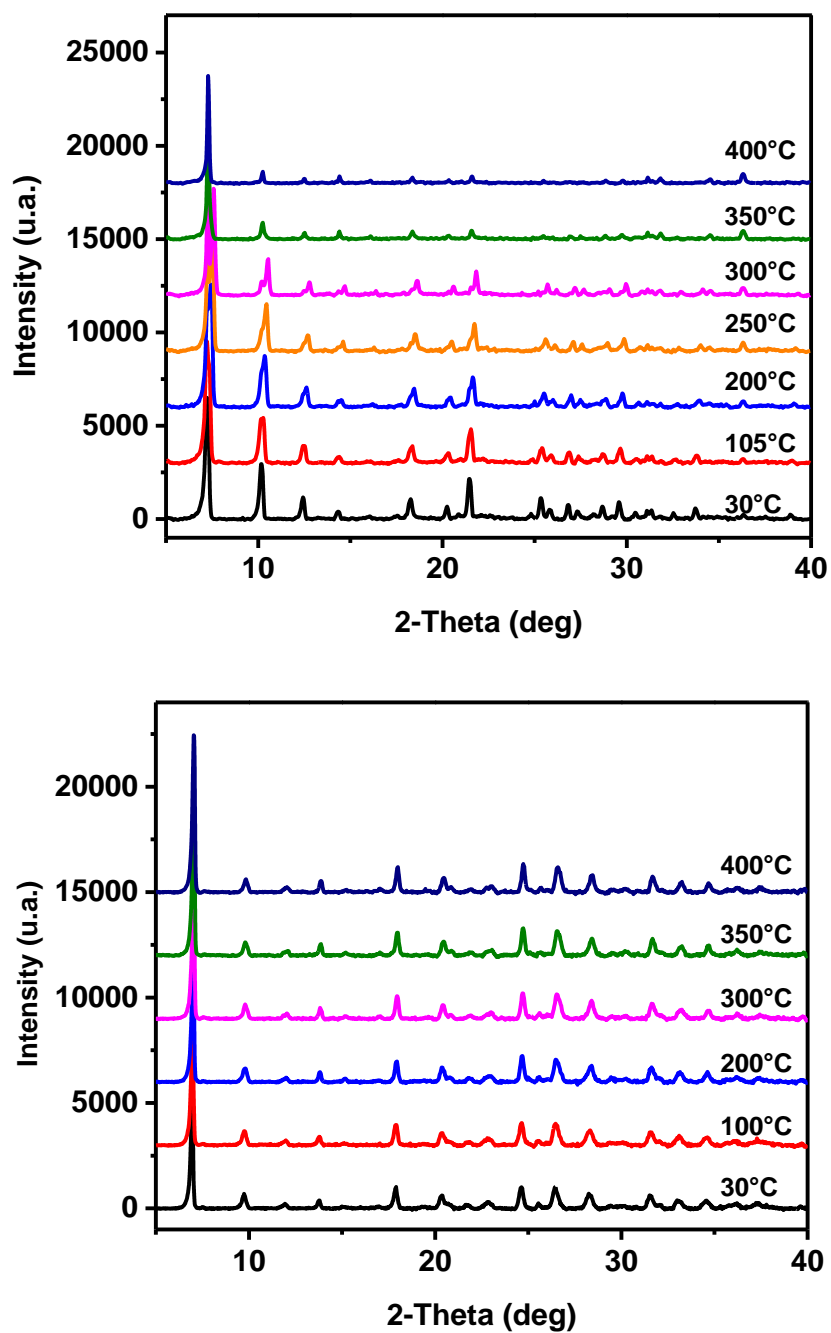


Figure S2. Variable temperature PXRD of **1** (top) and **2** (bottom) exhibiting their high thermal stability.

6. TGA analysis

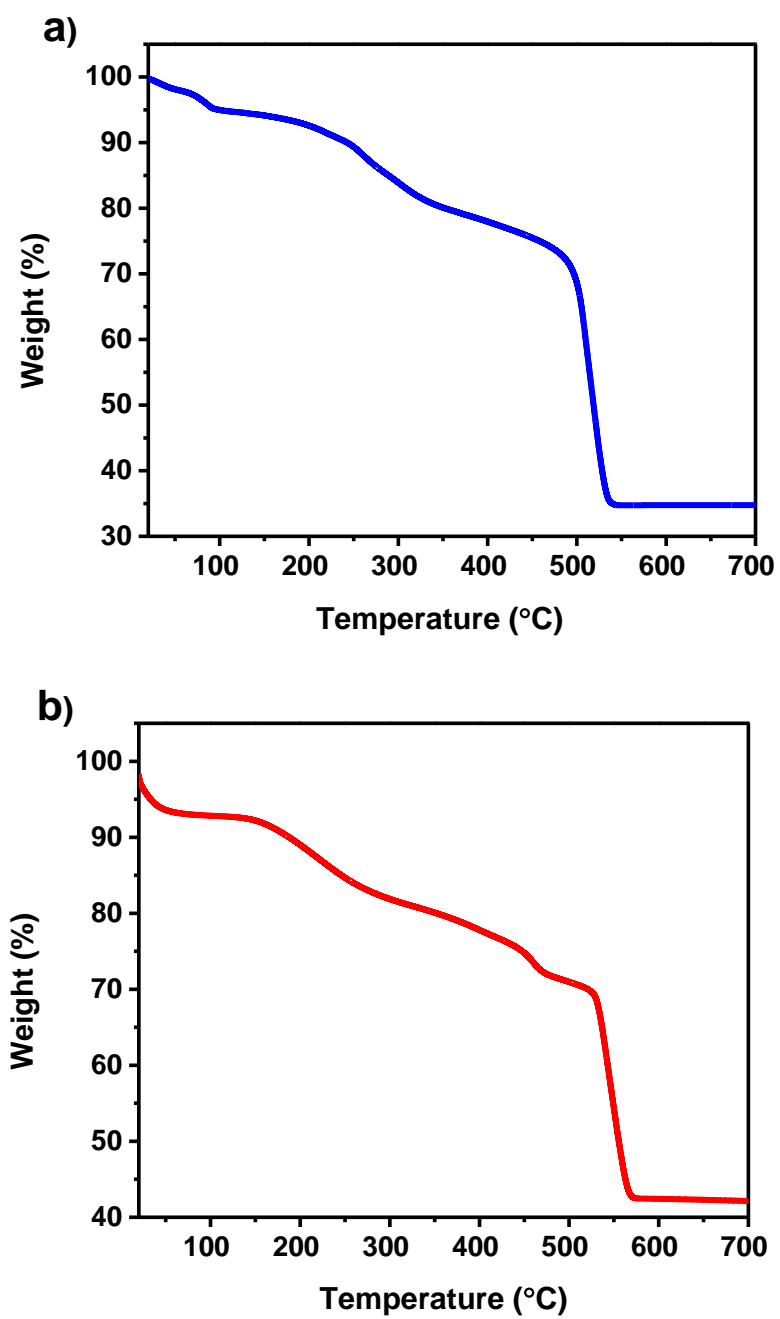


Figure S3. TGA plots of a) ethanol exchanged 1 and b) methanol-exchanged 2.

7. Low-Pressure Gas Adsorption Measurements

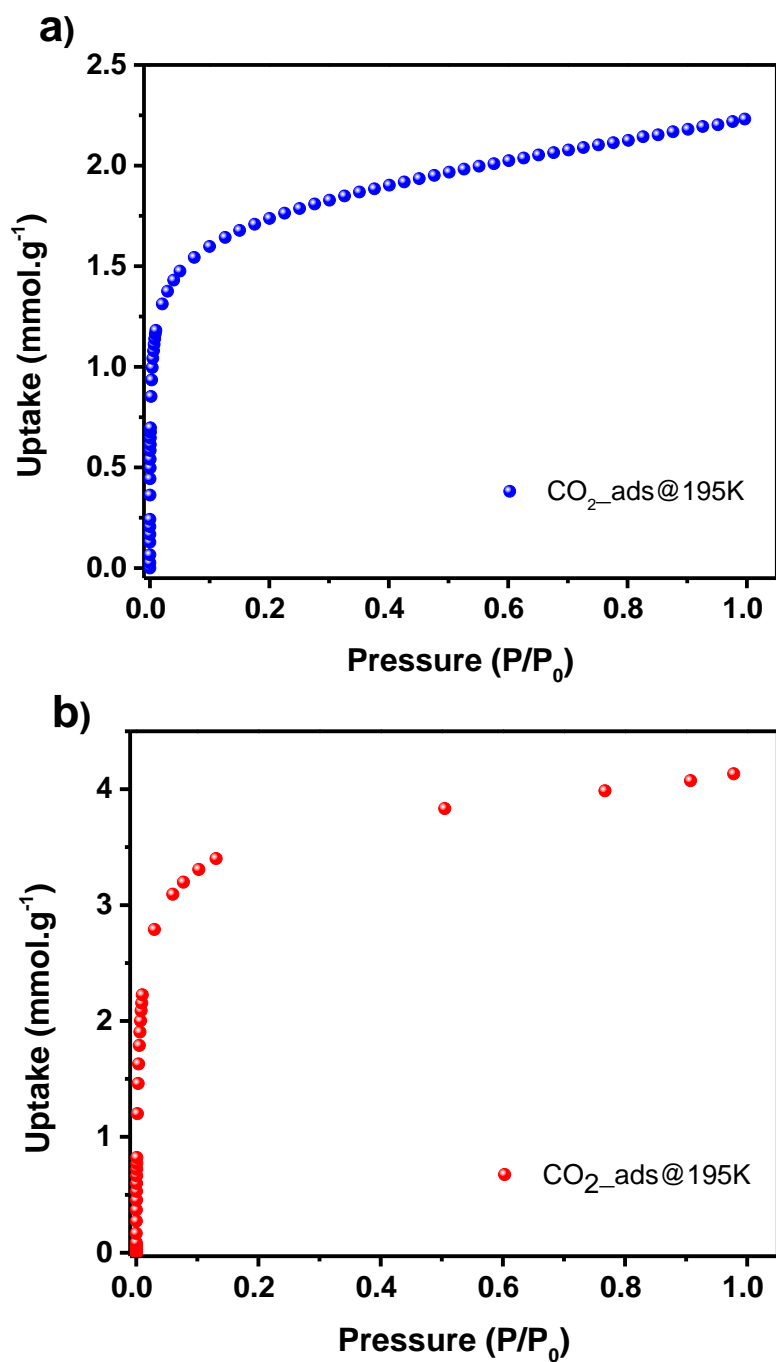
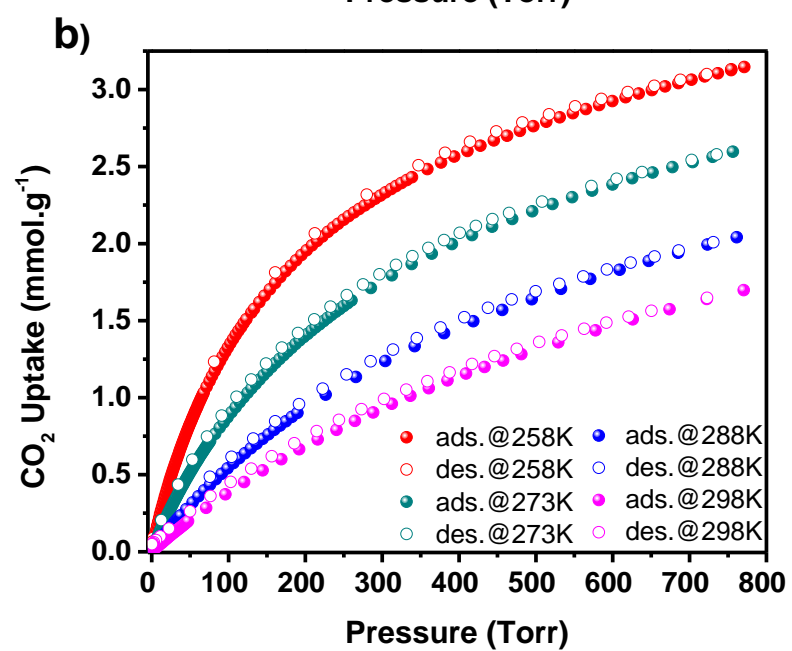
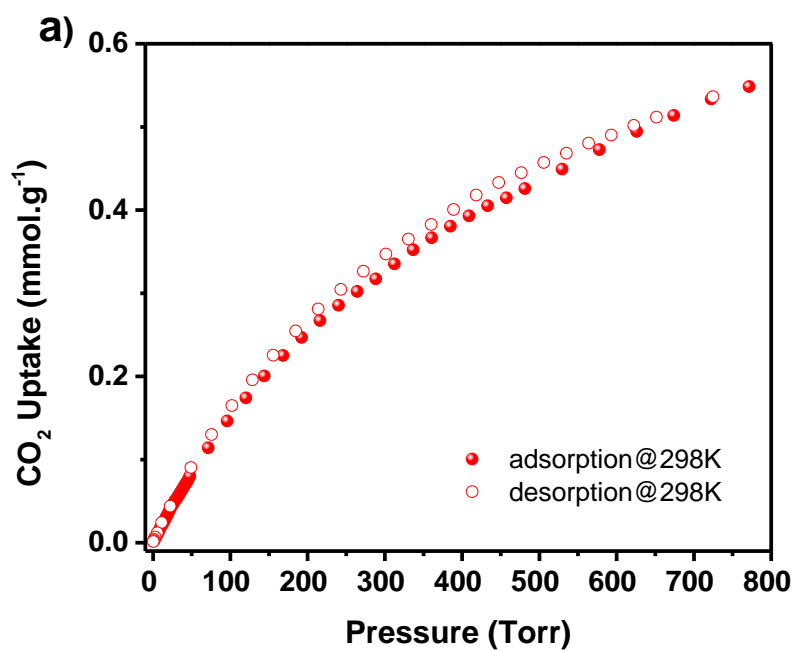


Figure S4. CO₂ adsorption isotherms collected at 195K for 1 a) and 2 b).



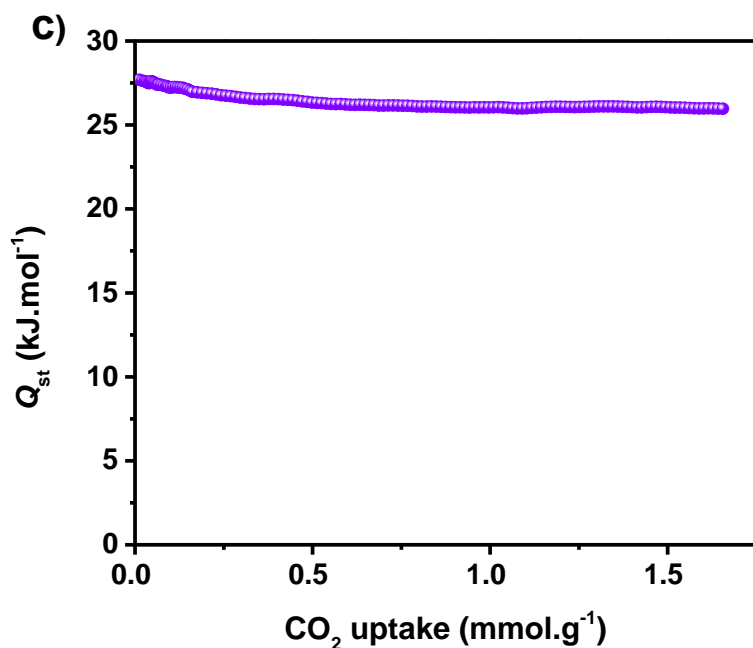


Figure S5. CO₂ sorption data for **1** and **2**: a) reversible CO₂ isotherm at 298K for **1**, b) fully reversible variable-temperature CO₂ isotherms of **2** and c) Q_{st} for CO₂ calculated from the corresponding isotherms for **2**.

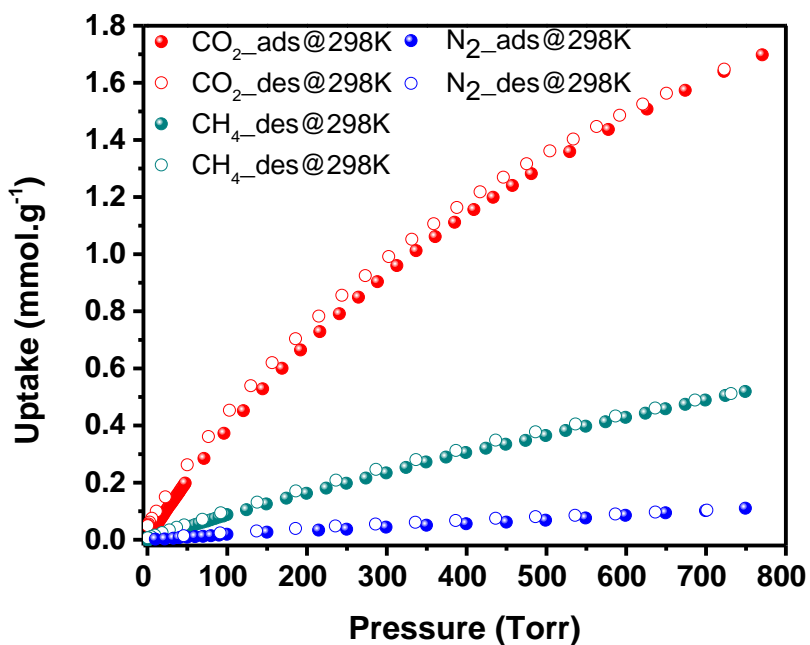
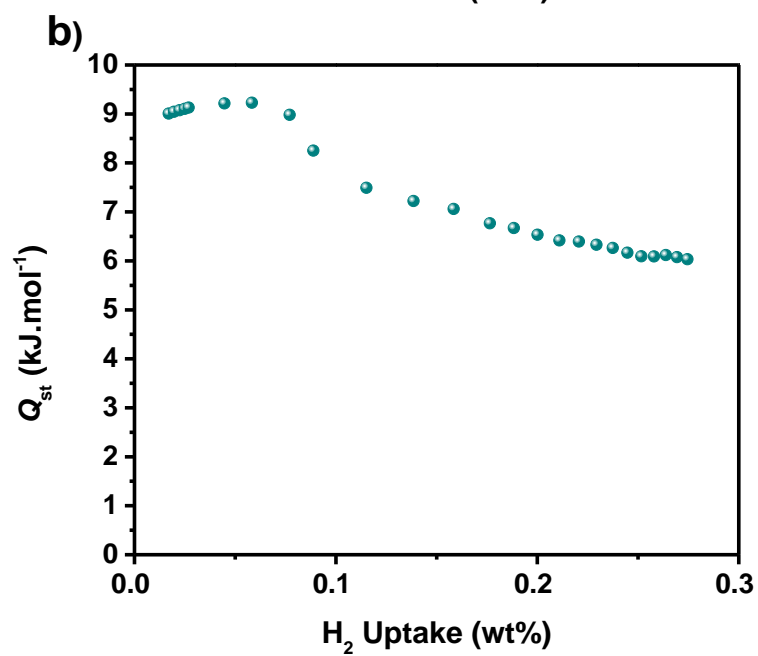
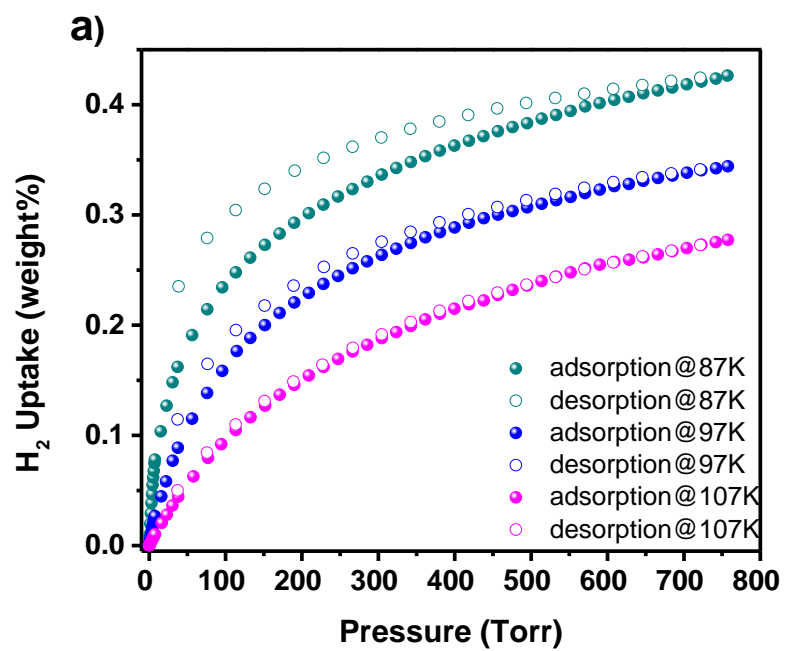


Figure S6. CO₂, CH₄ and N₂ sorption data for **2** at 760 torr and 298 K to display the selective adsorption towards CO₂ than CH₄ and N₂.



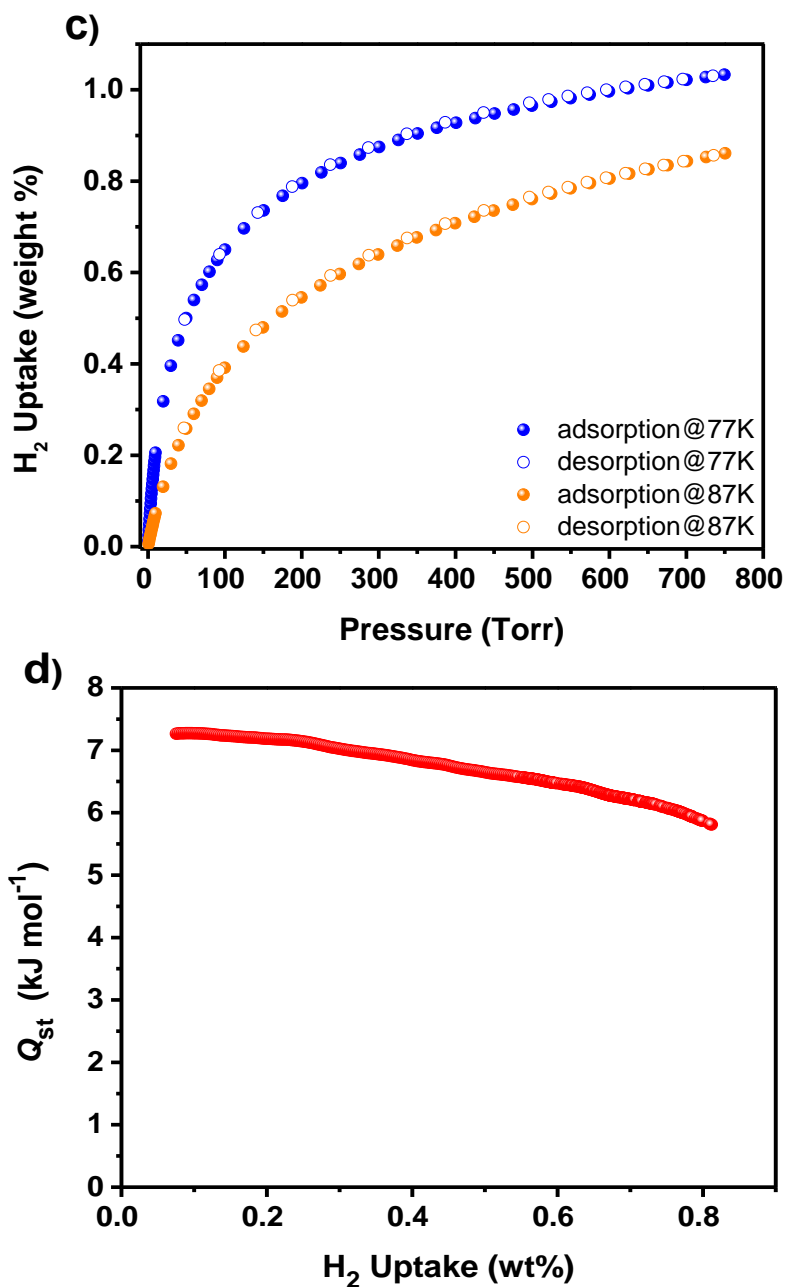


Figure S7. H₂ sorption data for data for **1** and **2**: a) fully reversible H₂ isotherms collected at 87, 97 and 107K and b) Q_{st} for H₂ calculated from the corresponding isotherms for **1** c) fully reversible H₂ isotherms collected at 77 and 87 K and d) Q_{st} for H₂ calculated from the corresponding isotherms for **2**.

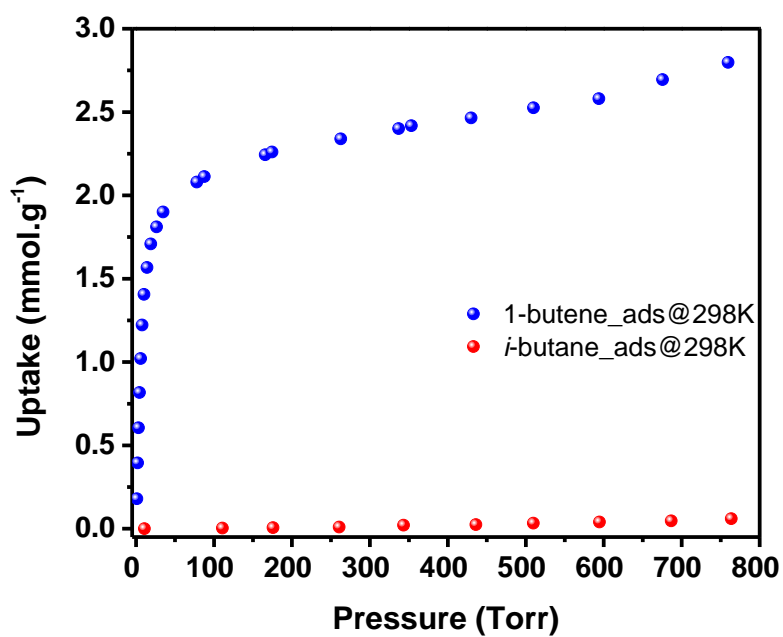


Figure S8. 1-butene and *i*-butane sorption isotherms for **2** showing molecular sieving between the relevant two gases.

8. Breakthrough experiments

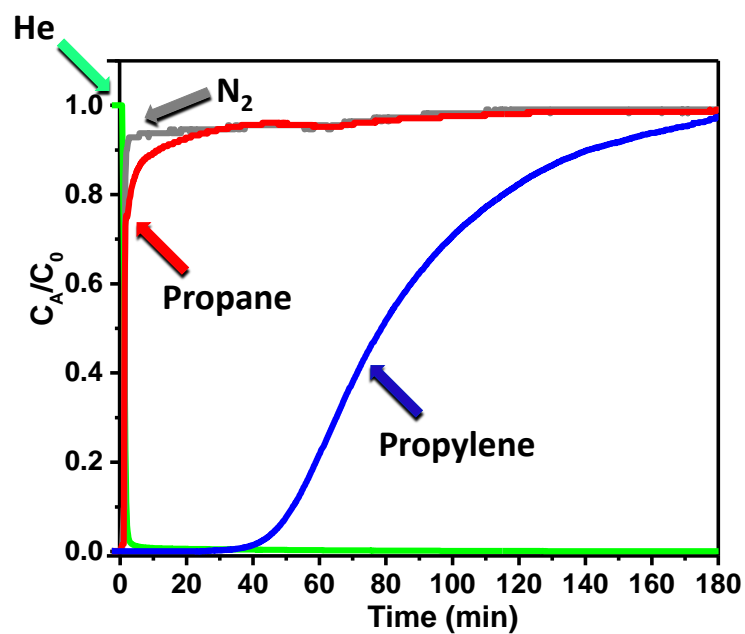


Figure S9. The breakthrough curve performed on **2** with a gas mixture of $C_3H_8/C_3H_6/N_2:5/5/90$ and a flow rate of 11 cc/min.

9. High-Pressure Gas Adsorption Measurements

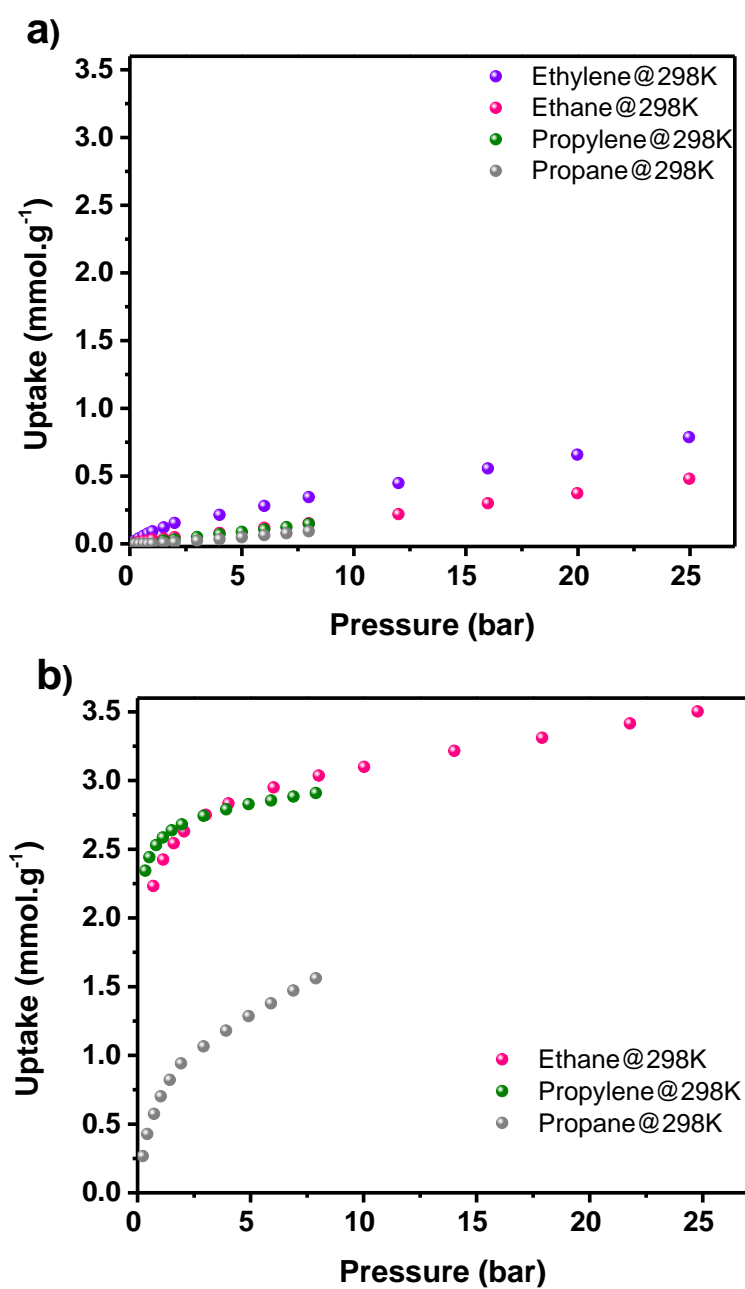


Figure S10. High pressure sorption isotherm for olefin and paraffin of a) 1 and b) 2.

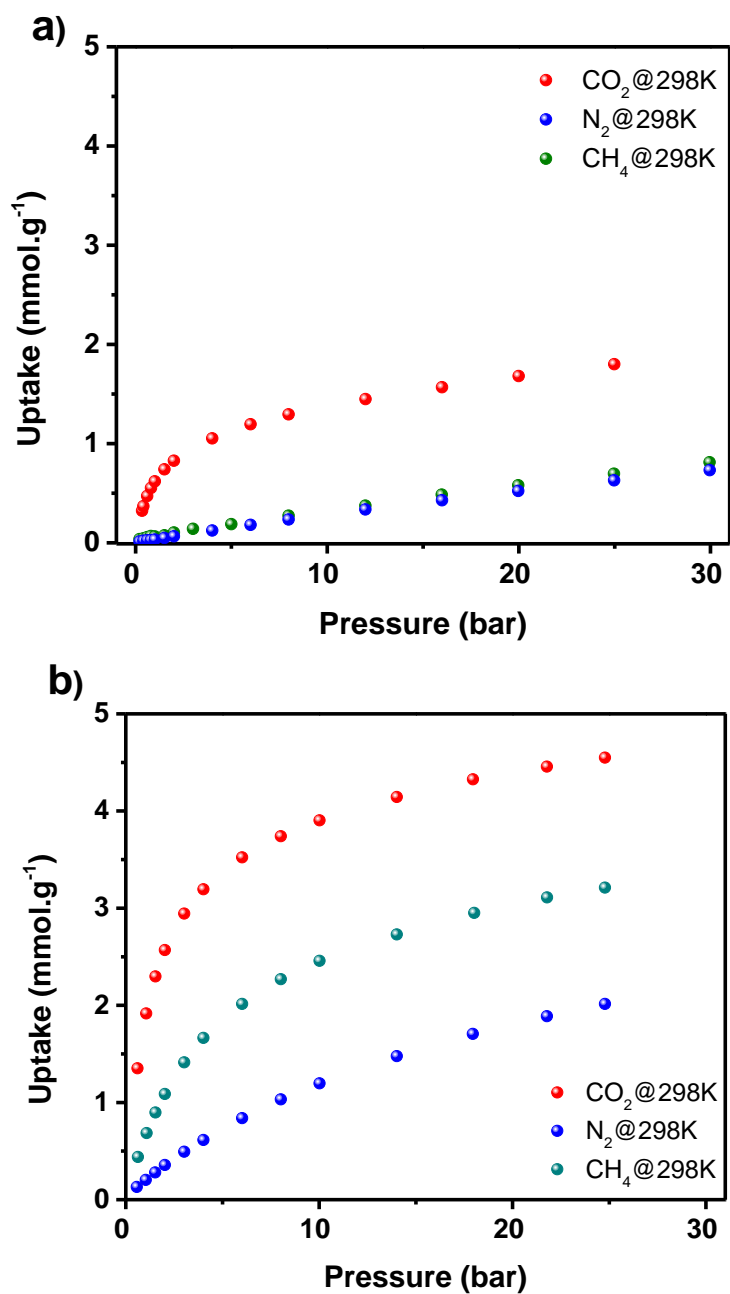


Figure S11. High pressure sorption isotherms of CO₂, N₂ and CH₄ at 298K for a) **1** and b) **2**.

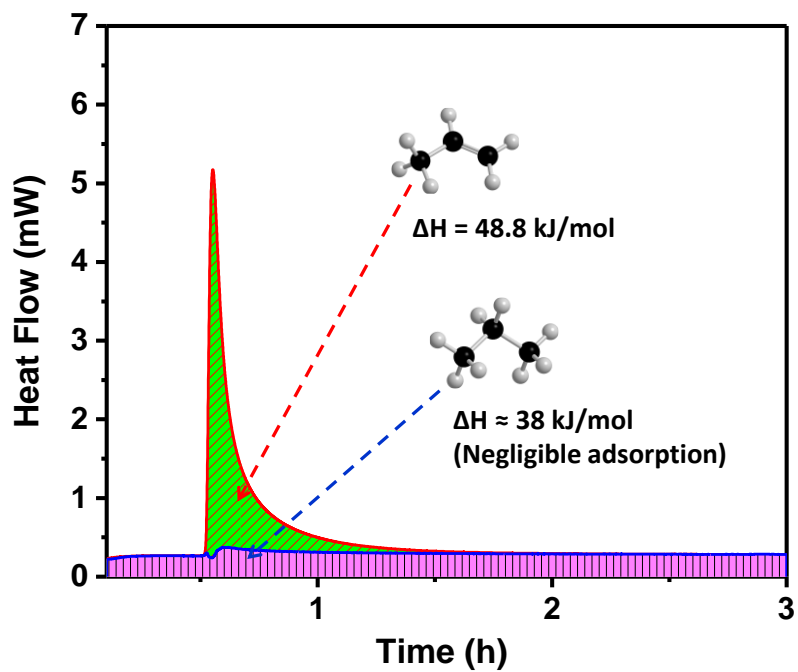


Figure S12. Simultaneous calorimetric and gravimetric measurements of C_3H_8 and C_3H_6 adsorption on **2** were performed to quantify the heat of adsorption of propylene and to reaffirm negligible adsorption of propane

10. References

- ¹ APEX2 (Bruker AXS Inc, Madison, Wisconsin, USA, 2014).
- ² SAINT (Bruker AXS. Inc, Madison, Wisconsin, USA, 2014).
- ³ SADABS (University of Gottingen, Germany, 2008).
- ⁴ Farrugia, L. WinGX suite for small-molecule single-crystal crystallography, *J. Appl. Cryst.*, **32**, 837-838, (1999); SHELXL-97 (1997); Sheldrick, G. M. Phase annealing in SHELX-90 - direct methods for larger structures, *Acta Cryst. A*, **46**, 467-473, (1990).
- ⁵ Dolomanov, O. V., Bourhis, L. J., Gildea, R. J., Howard, J. A. K. and Puschmann, H. *J. Appl. Cryst.* **2009**, *42*, 339-341.
- ⁶ Mazik, M.; König, A. *J. Org. Chem.* **2006**, *71*, 7854-7857.
- ⁷ Miller, S. R.; Alvarez, E.; Fradcourt, L.; Devic, T.; Wuttke, S.; Wheatley, P. S.; Steunou, N.; Bonhomme, C.; Gervais, C.; Laurencin, D.; Morris, R. E.; Vimont, A.; Daturi, M.; Horcajada, P.; Serre, C. *Chem. Commun.* **2013**, *49*, 7773-7775.